Impact of Virtual Oscillator Control on the instantaneous properties of VSC output voltage in distorted island grids

Mathias Melby[1], Marta Molinas[2*] and Olav Fosso[1]
[1] Department of Electric Power Engineering, Norwegian University of Science and Technology, Norway
[2] Department of Engineering Cybernetics, Norwegian University of Science and Technology, Trondheim, Norway
*E-mail: marta.molinas@ntnu.no

***Abstract*—This paper investigates the instantaneous properties of voltage and frequency of Voltage Source Converters (VSCs) when they are controlled by Virtual Oscillator Controllers (VOC) in a distorted island grid. Under time-averaged measurements, the VOC exhibits well known linear droop characteristics, which make them a good candidate for control in island grids. However, the instantaneous properties of VOC are influenced by the non-linear dynamics of the Van der Pol oscillator and provide better synchronization properties under distorted voltage conditions compared to the conventional droop controller. This is shown in a simulation study of parallel operation of two inverters serving a non-linear load that reveals a more stable synchronization at the expense of voltage quality in the case of the VOC compared to the conventional droop controller. These results provide convincing evidence for the adoption of a more complex controller as the VOC in island grids that will naturally be more vulnerable to voltage distortions. At the same time, these results encourage further explorations into other potential benefits of VOC in island grids.**

***Index Terms*—Virtual oscillator control, instantaneous frequency, droop controller, non-linear oscillator, island grids**

I. Introduction

Synchronization in island electrical grids dominated by power electronics is challenged by the absence of a grid reference to follow, lack of inertial sources and the usual lack of communication among the units. Most of the existing inverter controllers are grid-following and without an external grid the inverters need to determine the voltage and the frequency of the grid themselves. The droop control is the prevailing method for controlling inverters in a decentralized control architecture, where in a similar fashion to a synchronous generator, it regulates voltage and frequency linearly to variations of average reactive and active powers respectively [1] [2]. Droop controllers will then enable inverters to synchronize and share the load according to their output set points. The virtual oscillator control (VOC) has been proposed as an alternative to the droop control for improving the synchronization properties of inverters in island grids, by controlling them as Van der Pol oscillators. Through the electrical coupling between the inverters, the nonlinear oscillators synchronize and share the load according to their ratings [3]. The method is applicable for both single phase and three phase inverter systems [4]. Even though the VOC exhibits droop-like characteristics [5] [6] the method differs from conventional droop methods by acting to instantaneous changes instead of time-averaged measurements. This enables the VOC to offer better synchronization properties compared to the communication free droop alternative [7].

Earlier work has focused on the virtual oscillator control's possibility to synchronize faster than other available solutions. Depending on the system characteristics and the coupling strength between the inverters, the VOC will be able to outperform the droop control in terms of settling time following disturbances [7]. However, there has been limited interest into analyzing the effects the VOC could have on the overall voltage quality and on synchronization under highly distorted voltage conditions.

In this paper, the frequency and voltage properties of two parallel inverters controlled as Van der Pol Oscillators are analyzed. The synchronisation properties of the VOC and the droop controller are compared under distorted voltage conditions to show that the VOC achieves more stable synchronization at reasonable voltage quality while the droop controller is unable to sustain synchronization under the same distorted condition. Through analytic derivation of the instantaneous frequency expression and time-step simulations in MATLAB/Simulink, the impact of the oscillator parameters on the voltage quality and on synchronization is examined. The analysis is supported by developing a state-space representation of a microgrid consisting of two VO-controlled inverters serving a common load. By analyzing the dominant eigenvalues and how they depend on the parameters determining the voltage instantaneous properties, the inevitable trade-off between voltage quality and synchronization performance with the VOC is presented.

II. Microgrid Model investigated

The system configuration used in this study for the simulation investigation is schematically shown in Fig. 1. The level of detail of the model is set according to a realistic version with a time frame ranging from milliseconds and up to a few seconds. The source of power in the grid are two direct voltage sources each representing a PV panel with associated energy storage systems. Such power sources will typically have a larger time constants than the focus in this paper and they are therefore modeled as constant voltage sources. Since the

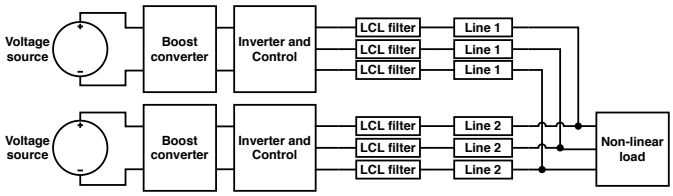

Fig. 1: A schematics of the microgrid composed of two inverters in parallel feeding a common non-linear load

voltage amplitude of the generation unit in a real situation will vary according to the weather conditions etc., a DC/DC boost converter is needed to transform the voltage into the required input level for the inverter. The boosted voltage will vary as the DC side capacitor is charged and discharged when power is drawn by the load. These voltage oscillations are, for this setup, well within the selected time frame and this behaviour is therefore implemented in the model. The main focus in this paper is the inverter control. The controllers give a voltage reference to a pulse width generator which controls the inverter switches. These switches are assumed ideal and set to turn on/off at a frequency of 15 kHz. The voltage output is a direct result of this switching process and is filtered with an LCL filter to achieve a smooth sinusoidal waveform. The line out of the two inverters are of the same type but vary in length. The load is common for both inverters and is assumed to be non-linear. This non-linear load is implemented through a diode rectifier together with a smoothing capacitor and inductor. Further details of the model implementation are found in [8].

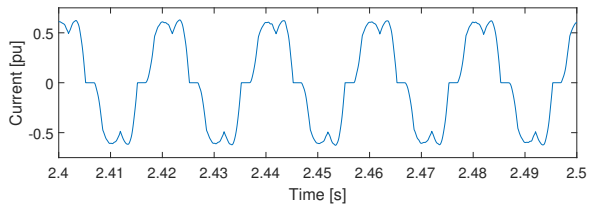

Fig. 2: Steady state load current.

A. Virtual Oscillator Controller: Van der Pol oscillator

Examples of interacting dynamical systems abound in science and technology, ranging from physics and chemistry, through biology and population dynamics, to communications and climate [9]. VSCs interacting in a microgrid is one such example of interacting electrical dynamical system. The VOC operating principle is based on the idea of controlling VSCs so that they mimic the dynamics of a non-linear oscillator as they are presumed to provide robust synchronization properties [10]. By doing that, the inverters would synchronize in similar way as network of coupled oscillators. There are several mathematical representations of the dynamics of non-linear oscillators and some of them have been used to describe the synchronization dynamics of coupled oscillators found in Nature [11] [12]. The Van der Pol oscillator [13], is one of such

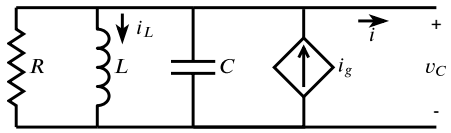

Fig. 3: Diagram of the Van der Pol oscillator. $i_g = -\alpha v_C^3$, and $R = -1/\sigma$.

representations and is adopted in this paper as the base for the virtual oscillator controller because it can produce stable limit-cycle oscillations. The synchronization and stability properties of this oscillator have been thoroughly investigated in island grids composed of single and multiple inverters feeding a resistive load under sinusoidal voltage conditions by Brian Johnson et. al in [7], [3], [14] and [15]. However, the properties of the VOC have not been thoroughly investigated under distorted and/or unbalanced voltage conditions.

The virtual oscillator control is shown in Fig. 4 and its dynamics are described by the circuit equations given as

$$\frac{di_L}{dt} = \frac{v_C}{L}, \qquad \frac{dv_C}{dt} = \frac{1}{C}\left(\sigma v_C - i_L - \alpha v_c^3 - K_i i\right) \quad (1)$$

To simplify, the following designations are defined

$$\epsilon = \sqrt{\frac{L}{C}}, \quad \omega^* = \frac{1}{\sqrt{LC}}, \quad \tau = \frac{t}{\sqrt{LC}} = \omega^* t \quad (2)$$

By developing the dynamics of the virtual oscillator in (1), the governing Van der Pol equation can be obtained as

$$\frac{d^2 v_C}{d\tau^2} - \epsilon\sigma\left(1 - 2v_C^2\right)\frac{dv_C}{d\tau} + v_C = -\epsilon K_i \frac{di}{d\tau} \quad (3)$$

This oscillator has a non-linear damping that is negative when v_C is small and positive when v_C is large. This way, the oscillations are restricted within an area around the fixed point and a limit-cycle is obtained. This means it will approach a periodic steady state. Further, by selecting suitable model parameters, the oscillations can achieve near-sinusoidal behaviour with a close to constant period and amplitude.

Presented in [15], a rotational matrix is utilized to be able to change between a conventional droop and a reversed droop characteristic for the VOC. The conventional $P-f$ and $Q-V$ relationship is obtained by selecting $\Phi = \pi/2$ in (4).

$$\Xi = \begin{bmatrix} cos(\Phi) & sin(\Phi) \\ -sin(\Phi) & cos(\Phi) \end{bmatrix} \quad (4)$$

In order to obtain a three phase voltage reference from the single phase oscillator, the Clarke Transform and its inverse form given in (5) is used. The inductor current i_L is orthogonal to v_C, which makes the scaled version $\omega^* L i_L$ the designated second input to the transformation. The final reference voltage for the inverter is obtained by scaling the transformed signal with the voltage gain K_v.

$$\begin{bmatrix} u_a \\ u_b \\ u_c \end{bmatrix} = \begin{bmatrix} 1 & 0 & 1 \\ -\frac{1}{2} & \frac{\sqrt{3}}{2} & 1 \\ -\frac{1}{2} & -\frac{\sqrt{3}}{2} & 1 \end{bmatrix} \begin{bmatrix} u_\alpha \\ u_\beta \\ u_0 \end{bmatrix} \quad (5)$$

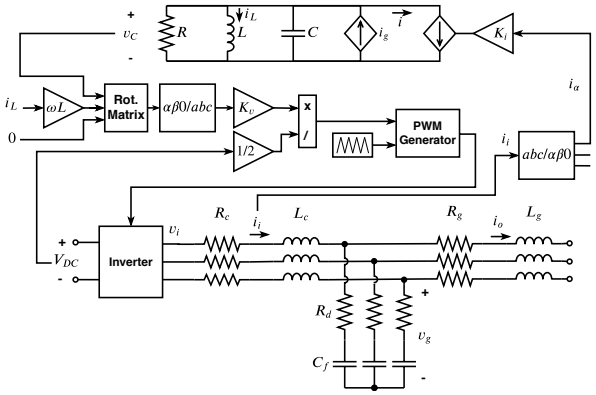

Fig. 4: Diagram of the virtual oscillator controller

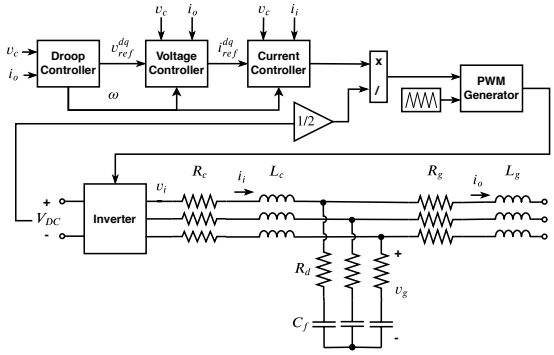

Fig. 5: Diagram of the conventional droop controller

By parameterizing the scaled capacitor voltage as

$$K_v v_C(t) = \sqrt{2}V(t)cos(\omega^* t + \theta^*(t)) \tag{6}$$

where ω^* is the nominal frequency and θ^* is the phase offset with respect to $\omega^* t$, the amplitude and phase dynamic of the oscillator are derived in [5] as

$$\begin{aligned}\frac{dV}{dt} &= \omega^*\epsilon\left(\sigma V cos(\phi) - \frac{2\alpha}{K_v^2}V^3 cos^3(\phi) - \frac{K_i K_v i}{\sqrt{2}}\right)cos(\phi)\\ \frac{d\theta^*}{dt} &= -\frac{\omega^*\epsilon}{V}\left(\sigma V cos(\phi) - \frac{2\alpha}{K_v^2}V^3 cos^3(\phi) - \frac{K_i K_v i}{\sqrt{2}}\right)sin(\phi)\end{aligned} \tag{7}$$

Here, the phase angle $\phi = \omega^* t + \theta^*$ is used.

B. Droop Controller

The conventional droop control implemented to control the inverter is realized by emulating the droop characteristic of synchronous generators in a traditional grid by controlling the output voltage and frequency of the VSC according to the variation of the output power [16]. The peer-to-peer droop control modality which does not require communication is adopted in this paper. The adopted version has three controllers which constitutes the droop control method. They are the droop controller, the voltage controller, and the current controller as illustrated in Fig. 5. The first part of the chain is the droop controller which gives a reference to the voltage controller based on the measured power output. The voltage controller is a faster unit which enables more precise control of the voltage over the capacitor. The current controller is the fastest controller which provides the final reference voltage for the inverter to follow. This control scheme ensures that the voltage reference for the inverter contains inherent characteristics to suppress harmonics caused in the inverter's switching process. This yields a more ideal output voltage than if only the droop block was implemented.

C. Instantaneous Frequency

In classical electric power systems, the frequency of the voltage is defined as the number of cycles per unit time. This is meaningful only for stationary signals which can be represented as a sum of stationary sines and cosines with constant frequencies. The assumption of a constant frequency in electric power systems has been valid since the power production traditionally has been dominated by large synchronous generators. This made possible the use of fast fourier transform (FFT) in the analysis and quantification of voltage quality by calculating the total harmonic distortion (THD). As power electronics are becoming more pervasive in the electric grid, ideal sinusoidal conditions cannot longer be guaranteed and it can be beneficial to evaluate the instantaneous properties of the grid voltage. To assess the impact of the VOC on the instantaneous properties of the VSC output, we first calculate and evaluate the instantaneous frequency of the reference voltage produced by the VOC. The instantaneous frequency, defined in [17] as

$$f_i = \frac{1}{2\pi}\frac{d\phi}{dt} = \frac{1}{2\pi}\frac{d}{dt}(\omega^* t + \theta^*) \tag{8}$$

can be derived for the virtual oscillator dynamics in (7) as

$$\begin{aligned}f_i = f^*\Bigg[1 - \frac{\epsilon}{V}\Big(\sigma V cos(\phi) - \frac{2\alpha}{K_v^2}V^3 cos^3(\phi)\\ - \frac{K_i K_v i}{\sqrt{2}}\Big)sin(\phi)\Bigg]\end{aligned} \tag{9}$$

where f^* is the nominal frequency. The instantaneous frequency of the VOC can be visualized in Fig. 6, where the influence of the VOC parameter shows clearly a time-varying frequency characteristic as ϵ increases with respect to a base case value of ϵ [8]. Conversely, by reducing the value of ϵ the frequency converges to a constant value, as it will be the case of an ideal sine wave. The importance of this time-varying frequency rests on being an inherent part of the generation of the VSC voltage which will be a scaled version of the VOC voltage.

III. Instantaneous properties of VOC and VSC voltages

When the VOC and VSC voltages are evaluated by their instantaneous properties, the non-linear dynamics of the VOC becomes evident. The waveform and the frequency of the

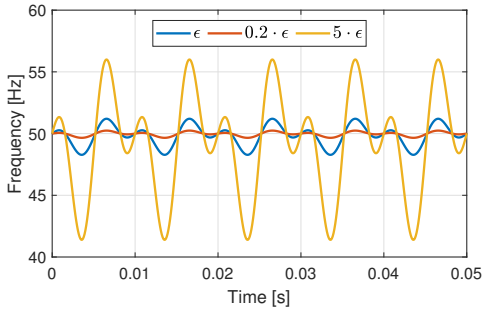

Fig. 6: Visualization of the analytical instantaneous frequency in (9) for the base case with $\epsilon = 0.011$ and variations of ϵ.

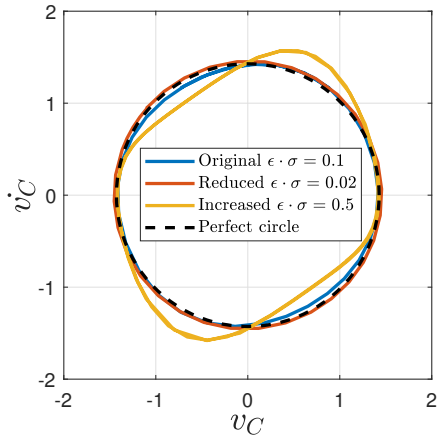

Fig. 7: Limit cycles for different parameters of the virtual oscillator.

capacitor voltage in the virtual oscillator depends on the parameters ϵ and σ as well as their product $\epsilon \cdot \sigma$. This is clear from (3) and (9). Phase portraits of the virtual oscillator's limit cycle with different values of $\epsilon \cdot \sigma$ are visualized in Fig. 7. The closer to a perfect circle, the closer to a perfect sine wave will the capacitor voltage be.

The impact of the value of ϵ on the instantaneous frequency is visualized in Fig. 6. The plot is made with the parameters in Table I and an RMS voltage $V = 240.06$ V and a current $i = \sqrt{2} \cdot 12.80 cos(\omega^* t + 1.32)$ A. The voltage and current information are obtained from time-step simulations of the virtual oscillator controlled inverter implemented in MATLAB.

	THD [%]	
ϵ	v_g	v_C
0.011	2.1	1.2
$0.2 \cdot 0.011$	2.0	0.3
$5 \cdot 0.011$	4.5	6.15

TABLE I: Total harmonic distortion for the voltage output, v_g, and the oscillator voltage, v_C, for different values of ϵ.

Fig. 8 shows the instantaneous VSC output voltage together with the VOC voltage. It is seen that the VOC voltage is less distorted than the reference voltage since the inductor current i_L which makes up the orthogonal component, is closer to an ideal sine wave.

To explore the impact of the oscillator parameters on the

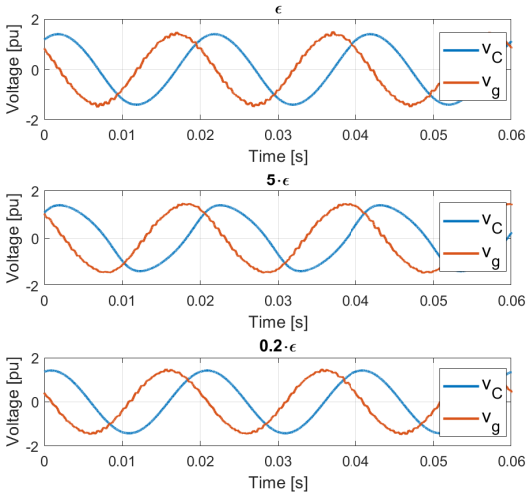

Fig. 8: Oscillator voltage, v_C, and output voltage, v_g, for the base case with $\epsilon = 0.011$ and variations of ϵ.

voltage quality and synchronization, an eigenvalue analysis is performed based on a state-space representation of the investigated system using the averaged model of the VOC [5]. The dependence of the trajectory of the dominant eigenvalues on the VOC parameters, shown in Figures 9 and 10 together with Fig. 7, indicates the inevitable trade-off between voltage quality and strength of synchronization with the VOC. By inspection of the plots, it is seen that as ϵ decreases, the distortion is attenuated while the stability margin is drastically reduced. Similar effects are found when σ decreases, but the reduction of the stability margin is not as large as with the decrease of ϵ.

Control method	Dominant poles
VOC	$\lambda = -18.236$ $\lambda = -15.166$ $\lambda = -9.680$
Droop	$\lambda = -45.502$ $\lambda = -31.950$ $\lambda = -31.421$ $\lambda = -12.675 \pm j15.472$

TABLE II: Dominant poles with the control methods. The remaining poles have real values < -400.

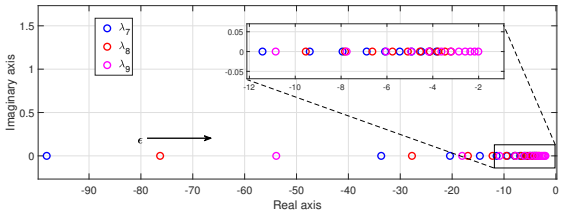

Fig. 9: Root locus plot when varying ϵ from 55.53e-3 to 2.22e-3. The horizontal arrow indicate the trajectory for the three dominant eigenvalues when ϵ is reduced. The base case eigenvalues can be found in II.

IV. Simulation Model and Results

A model corresponding to the system in Fig. 1 is implemented in MATLAB. The grid characteristics used in the

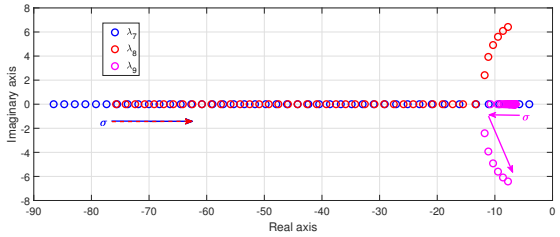

Fig. 10: Root locus plot when varying σ from 45.24 to 2.24. Two poles coincide and become complex conjugates when $\sigma < 7.9885$. The different colored markers and arrows show the trajectory of each of the dominant eigenvalues when σ is reduced. The base case eigenvalues are given in II.

Name	Symbol	Value
Nominal phase voltage	V^*	$400/\sqrt{3}$ V (RMS)
Nominal frequency	f^*	50 Hz
Rated active power	P_{rated}	10 kW
Rated reactive power	Q_{rated}	10 kVAR
Maximum voltage	V_{max}	242.287 V
Minimum voltage	V_{min}	219.393 V
Switching frequency	f_{sw}	15 kHz
Nominal DC side voltage	V_{DC}	750 V

TABLE III: System parameters for the microgrid implemented in the simulations.

simulations are described by the system parameters in Table III.

A. Virtual Oscillator Parameters

The virtual oscillator parameters are selected to be steady-state equivalent with the droop controlled inverter. The governing droop relations are

$$V = V_{max} - m_q Q, \qquad \omega = \omega^* - n_p P \tag{10}$$

The oscillator parameters are determined based on the droop coefficients, m_q and n_p, as well as the system parameters presented in Table III. The correlation between the droop controller and the virtual oscillator control have been presented in [5] which dictates that in order to have the equivalence between droop and VOC, the oscillator parameters, C and σ, should satisfy

$$C = \frac{1}{n_p}\frac{K_i}{6K_v}, \qquad \sigma = \frac{1}{m_q}\frac{K_i}{6} \tag{11}$$

Furthermore, the other parameters are selected as

$$K_v = V_{max}, \quad K_i = 3\frac{V_{min}}{Q_{rated}}, \quad \alpha = \frac{2}{3}\sigma, \quad L = \frac{1}{C(\omega^*)^2} \tag{12}$$

By setting the droop coefficients $n_p = 1.586 \cdot 10^{-4}$ and $m_q = 1.21 \cdot 10^{-3}$ and following the system parameters, the corresponding virtual oscillator parameters become as given in Table IV.

B. Simulation Results

Two different cases are simulated to investigate the speed and strength of synchronization. The first case considers a highly distorted voltage created by connecting a non-linear load with a typical grid coupling strength where $Z_{line,1} = 0.794 + j0.558\ \Omega$ and $Z_{line,2} = 2 \cdot Z_{line,1}$. The second case considers a lower voltage distortion which is achieved by reducing the coupling strength by setting $Z_{line,1} = 3.97 + j2.79\ \Omega$ and $Z_{line,2} = 7.94 + j5.58\ \Omega$.

Name	Symbol	Value
Voltage gain	K_v	242.287
Current gain	K_i	65.818×10^{-3}
Oscillator conductance	σ	9.048 S
Current source factor	α	6.032
Oscillator capacitance	C	286.562×10^{-3} F
Oscillator inductance	L	35.357×10^{-6} H

TABLE IV: Virtual oscillator parameters.

The simulation cases are made with one inverter initially connected and addition of a second inverter after steady state is achieved. The first case is with a load of $10.7 + j5.1$ kVA and inverter addition after 0.5 seconds, and the second case with a load of $4.0 + j1.3$ kVA and inverter addition after 0.8 seconds.

Fig. 11 shows the instantaneous responses of load voltage, the synchronization index of the inverter output currents (equal to the projector matrix in [14]) and the THD for both the VOC and droop control under highly distorted voltage conditions and strong grid coupling. In this case, the conventional droop control cannot sustain a stable synchronization while the VOC exhibits good properties.

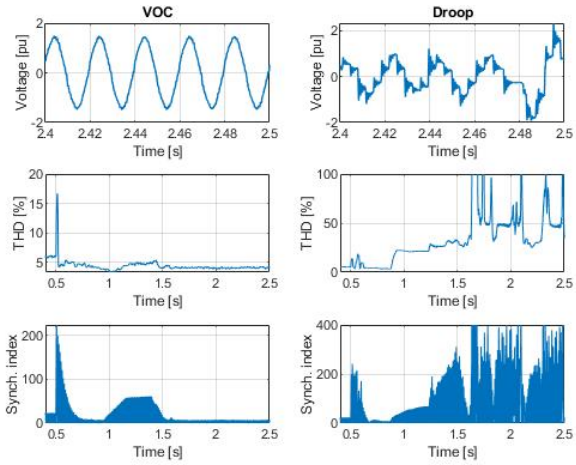

Fig. 11: Instantaneous load voltage, THD and Synchronisation index for VOC and droop control under strong grid coupling.

When the voltage distortion is reduced by lowering the coupling strength, the droop controller sustains synchronization with very similar properties as the VOC. This case is illustrated in Fig. 12, which shows the instantaneous responses of voltage, THD and synchronization index for the conventional droop controller and the VOC. The speed of synchronization under this case appears to be the same for both the droop control and the VOC.

The THD of the load voltages in Figures 11 and 12 is

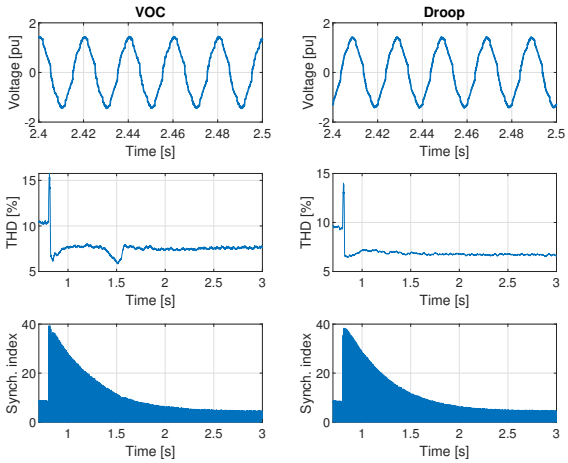

Fig. 12: Instantaneous responses of load voltage, THD and Synchronization index for the VOC and Droop control under weaker grid coupling.

calculated as

$$\text{THD} = \frac{1}{3}\sum_{j=1}^{3}\text{THD}_j = \frac{\sqrt{V_{j2}^2 + V_{j3}^2 + V_{j4}^2 + \ldots}}{V_{j1}} \qquad (13)$$

where V_{ji} is the RMS value of the instantaneous value of the i-th quasi-harmonic component of the j-phase voltage. The fundamental frequency was set equal to the average frequency, 49.9 Hz and the sampling frequency was 400 kHz.

V. Concluding Remarks and Future Work

This paper has examined the impact that controlling a VSC with a VOC has on the instantaneous properties of both the reference voltage generated by the VOC and the output voltage of the VSC. In order to have a reference for evaluating this impact, a conventional droop control is implemented and compared to the VOC in terms of synchronization. The impact of the VOC is further evaluated comparing the time required for synchronization and the strength of synchronization when using the VOC and the droop control. The results of this preliminary investigation indicates that when compared to the conventional droop control, the VOC exhibits very robust synchronization properties under highly distorted voltage conditions. It is observed that in order to achieve similarly robust synchronization with the droop control, the grid coupling strength has to be lowered. The following general observations can be made from these results:

- a weak coupling between inverters favors robust synchronization with droop controlled inverters under distorted voltage conditions
- robust synchronization with VOC can be achieved under a wider range of coupling strength at the expense of voltage quality
- under highly distorted voltage conditions the VO-controlled inverters can sustain robust synchronization while the conventional droop control is unable

These results are to some extent expected since the conventional droop control is an average value-based controller while the VOC is acting on instantaneous information about the grid. Therefore, the strength of the VOC is more evident under distorted voltage conditions where the conventional droop shows its weakness. Further work will expand the operation under non-ideal grid conditions by including unbalanced voltage and will compare the VOC with a modified droop controller that takes instantaneous information of active and reactive powers, changing the linear droop characteristics into a non-linear droop.

References

[1] J. P. Lopes, C. Moreira, and A. Madureira, "Defining control strategies for microgrids islanded operation," *IEEE Transactions on power systems*, vol. 21, no. 2, pp. 916–924, 2006.

[2] F. Katiraei and M. R. Iravani, "Power management strategies for a microgrid with multiple distributed generation units," *IEEE transactions on power systems*, vol. 21, no. 4, pp. 1821–1831, 2006.

[3] B. B. Johnson, S. V. Dhople, A. O. Hamadeh, and P. T. Krein, "Synchronization of parallel single-phase inverters with virtual oscillator control," *IEEE Transactions on Power Electronics*, vol. 29, no. 11, pp. 6124–6138, 2013.

[4] B. B. Johnson, S. V. Dhople, J. L. Cale, A. O. Hamadeh, and P. T. Krein, "Oscillator-based inverter control for islanded three-phase microgrids," *IEEE Journal of Photovoltaics*, vol. 4, no. 1, pp. 387–395, 2013.

[5] M. Sinha, F. Dörfler, B. B. Johnson, and S. V. Dhople, "Uncovering droop control laws embedded within the nonlinear dynamics of van der pol oscillators," *IEEE Transactions on Control of Network Systems*, vol. 4, no. 2, pp. 347–358, 2017.

[6] Z. Shi, H. I. Nurdin, J. E. Fletcher, and J. Li, "Similarities between virtual oscillator controlled and droop controlled three-phase inverters," in *2018 IEEE 18th International Power Electronics and Motion Control Conference (PEMC)*. IEEE, 2018, pp. 434–439.

[7] B. Johnson, M. Rodriguez, M. Sinha, and S. Dhople, "Comparison of virtual oscillator and droop control," in *2017 IEEE 18th Workshop on Control and Modeling for Power Electronics (COMPEL)*. IEEE, 2017, pp. 1–6.

[8] M. Melby, "Comparison of virtual oscillator control and droop control in an inverter-based stand-alone microgrid," Master's thesis, NTNU, published 07.06.2019. Will be available online.

[9] A. Winfree, *The Geometry of Biological Time*, ser. Biomathematics (Berlin). New York, 1980.

[10] S. V. Dhople, B. B. Johnson, and A. O. Hamadeh, "Virtual oscillator control for voltage source inverters," in *2013 51st Annual Allerton Conference on Communication, Control, and Computing (Allerton)*, 2013, pp. 1359–1363.

[11] L. Schimansky-Geier, "Kuramoto, y., chemical oscillations, waves, and turbulence. berlin-heidelberg-new york-tokyo, springer-verlag 1984. viii, 156 s., 41 abb., dm 79,â. us $ 28.80. isbn 3-540-13322-4 (springer series in synergetics 19)," *ZAMM - Journal of Applied Mathematics and Mechanics / Zeitschrift fÃ¼r Angewandte Mathematik und Mechanik*, vol. 66, no. 7, pp. 296–296, 1986.

[12] S. Strogatz, *Sync: The Emerging Science of Spontaneous Order*. Hyperion Books, 2003.

[13] T. Kanamaru, "Van der Pol oscillator," *Scholarpedia*, vol. 2, no. 1, p. 2202, 2007, revision #138698.

[14] B. B. Johnson, M. Sinha, N. G. Ainsworth, F. Dörfler, and S. V. Dhople, "Synthesizing virtual oscillators to control islanded inverters," *IEEE Transactions on Power Electronics*, vol. 31, no. 8, pp. 6002–6015, 2015.

[15] M. Sinha, S. Dhople, B. Johnson, N. Ainsworth, and F. Dörfler, "Nonlinear supersets to droop control," in *2015 IEEE 16th Workshop on Control and Modeling for Power Electronics (COMPEL)*. IEEE, 2015, pp. 1–6.

[16] F. Li, R. Li, and F. Zhou, *Microgrid technology and engineering application*. Elsevier, 2015.

[17] B. Boashash, "Estimating and interpreting the instantaneous frequency of a signal. i. fundamentals," *Proceedings of the IEEE*, vol. 80, no. 4, pp. 520–538, 1992.